

Prediction of Matrix-Precipitate Interfacial Free Energies: Application to Al-Al₃Li *

Marcel Sluiter¹, Mark Asta², and Yoshiyuki Kawazoe¹

¹ *Institute for Materials Research, Tohoku University, Sendai 980-77 Japan*

² *Sandia National Laboratory, Livermore, CA 94551, USA*

(Received November 14, 1995)

Many aspects of the behavior of bulk materials are determined by the properties of interfaces. In the field of metallurgy, for example, the interfacial free energy is a crucial factor in the theory of the nucleation, growth, and morphology of precipitates. So far the complexity associated with the inherent disorder at an interface has eluded the ab-initio computation of its free energy and other thermodynamic properties. Here, we show that a particular type of interface can be modeled from first-principles with remarkable accuracy by combining the statistical thermodynamics of the Ising Hamiltonian with the zero-temperature energetics from ab-initio local-density-functional electronic structure calculations.

KEYWORDS: interfacial energy, Al-Li alloys, alloy theory, cluster variation method

1. Introduction

The theory of interfacial thermodynamics was first studied in a continuum approximation over a century ago by van de Waals [1] and later by Cahn and Hilliard [2]. Since this pioneering work there have been numerous studies which take into account the discreteness of the lattice through the use of idealized models [3]. Recently, the study of interface specific phenomena with more accurate models has received renewed attention [4, 5].

In all studies conducted so far, the energetic interaction parameters between different atomic species have been selected either arbitrarily [4, 5], or by fitting to some experimentally measured properties [3]. Here, the energetic parameters for Al-Li alloys have been obtained with a variant of the Connolly-Williams method [6] from the electronic total energies [7] of a small set of ordered superstructures. Hence, the current description is predictive and has no adjustable parameters.

In this work the interface that exists between two phases in chemical equilibrium, a so-called interphase boundary (IPB), has been studied. The two phases have the following features: 1) they have the same lattice parameters, 2) one phase is a disordered fcc solid solution, and 3) the other phase is ordered with the L1₂ (Cu₃Au type) crystal structure. These features describe accurately the nature of the IPBs between the Al-rich fcc matrix and the metastable δ' precipitates in technologically important Al-Li alloys.

A supercell which models such an IPB on the (100) plane is shown in figure 1. On the bottom the δ' phase is represented. Its crystal structure can be easily visualized by an fcc cube where the cube corners (face centers) are occupied mostly by Li (Al) atoms. At the top, in the fcc solid solution, all sites have equal probability of being occupied by the Li species. In the middle a transition region occurs where, going from bottom to top, the distinction in occupancy of the cube

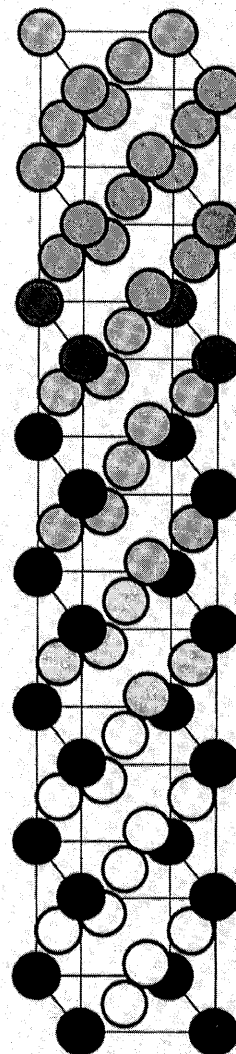


Figure 1: Supercell with a (100) IPB. The actual supercell used in CVM calculations consists of 38 fcc cubes. White (black) spheres represent Al(Li) atoms, and grey spheres indicate mixed atomic occupancy.

*IMR Report No. 1996.

corner and face center sites gradually disappears. At very low temperatures the disappearance may be sharp rather than gradual. If vibrational and electronic excitations are ignored, the thermodynamic properties of such a supercell can be examined with the Ising model. The partition function pertaining to the Ising Hamiltonian cannot be solved exactly for such complicated 3-dimensional configurations, but accurate approximations are obtained with the tetrahedron-octahedron cluster variation method (CVM) of Kikuchi [4]. Solving the partition function yields the composition profile and the thermodynamic properties of the supercell. The properties of IPBs are obtained by subtracting properties of the bulk system without IPBs from those pertaining to the supercell.

2. Formalism

Total energies of a large number of fcc superstructures were computed with the LMTO-ASA method [7]. Equal sphere radii were selected for Al and Li, the "combined corrections" to the ASA were included, and the von Barth-Hedin parametrization of the exchange-correlation potential was used. Care was taken to compute all superstructures with the same k-point grid, which included 1000 points in the 1st Brillouin zone of the fcc crystal structure. Formation energies ΔE_{form} were extracted from the total energies E_{tot} by subtracting the concentration-weighted average of the total energies of the pure elements in the fcc state, according to

$$\Delta E_{form}^{\alpha} = E_{tot}^{\alpha} - c_{Li}^{\alpha} E_{tot}^{Li-fcc} - (1 - c_{Li}^{\alpha}) E_{tot}^{Al-fcc} \quad (1)$$

where the superscript α refers to a particular superstructure and c_{Li} is the concentration of the Li species.

Effective cluster interactions (ECI) from the total energies by means of a Connolly-Williams procedure [8]. The ECI J_i for a cluster i are calculated with

$$\sum_{\alpha} w^{\alpha} [\Delta E_{form}^{\alpha} - \sum_{i=1}^n J_i \xi_i^{\alpha}]^2 = \text{minimal} \quad (2)$$

where ξ is the cluster correlation function as defined in equation 10 in Ref. [9], and w represents the weights assigned to each structure. The weights are determined according to

$$w^{\alpha} = \frac{1}{1 + \omega \left(\frac{d_{\alpha}}{\langle d \rangle} \right)^2} \quad (3)$$

where d_{α} represents the distance of a structure α to the convex hull formed by the ground state ordered structures, and $\langle d \rangle$ is the distance averaged for all structures. Of course, d_{α} takes the value zero if α is a ground state. ω is a factor which is assigned the smallest positive value which insures that the total energies of all structures are in the correct order, as in the spirit of Ref. [10]. In the actual calculations ω was given the value 2.

The idea of weighting each structure is as follows: If a structure is very close, or right on the convex hull, it represents an atomic configuration that occurs with

high probability in the actual alloy, and hence it is important that this energy be described accurately. Some other structure that is far above the convex hull represents a configurations that is not very likely to occur in the actual alloy, and thus does not need to be described quite as accurately. Equation 2 was solved using a singular value decomposition procedure. The advantage of this method over the usual Connolly-Williams procedure is that in one calculation not only the values of the ECI are determined but, that in an underdetermined system one also finds at the same time the set of clusters $\{i\}$ which best describe the energetics of the alloy. We have checked that the cluster expansion thus obtained correctly orders the relative stabilities of all phases [10]. An additional benefit of weighting the lowest energy states more heavily in the Connolly-Williams method is that a much more rapid convergence of the cluster expansion is obtained. This has been noticed particularly in ionic systems [11]. The cluster expansion gives the formation energy of any decoration of the lattice, provided that its correlation functions are known:

$$\Delta E_{form}^{\alpha} = \sum_i \xi_i^{\alpha} J_i. \quad (4)$$

The convergence of the cluster expansion of the formation energy has been checked with the following procedure: A set of n ordered structures is selected. Using the "exact" (read: LMTO-ASA) formation energies of $n - 1$ ordered structures, the ECI are computed according to eq. 2. The ECI are then inserted in eq. 4 to compute the formation energy of the structure nr n , which has not been included in the calculation of the ECI, and the difference between the "exact" value and the ECI predicted value for the formation energy is computed; this difference is referred to as the "error of the predicted formation energy". This procedure is repeated so that each structure is excluded once, such that for each structure the error of the predicted formation energy is calculated. When the error averaged for all structures is greater than some tolerance, the expansion is considered to be unconverged and an LMTO-ASA calculation is carried out for a new structure. If this structure has a composition c_{Li} different from 0.5, both composition c_{Li} and $1 - c_{Li}$ are considered. This procedure is repeated until the error of the predicted formation energy is less than some tolerance. The procedure is started with the set of ground states stabilized by the nearest-neighbor effective pair interaction (EPI). The set has been expanded with other ground states [12, 13, 14] stabilized by more distant EPI, and also with some simple structures based on alternating occupancies on low index crystallographic planes. The following set of 14 structures has been used to extract the ECI: fcc, L1₀, L1₂, K40 [14], DO₂₂, C2/m AB₅ and A₂B₄ [15], and C11_b (MoPt₂ prototype), which gives an error in the predicted formation energy of 1.5 mRyd/atom corresponding to a relative error of about 20 %.

Both the Al-rich fcc solid solution and the δ' phase have the same lattice parameter of 0.4 nm. Therefore,

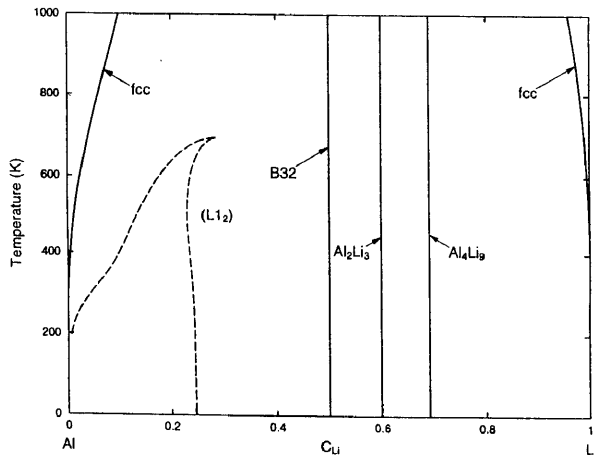


Figure 2: The solid state part of the computed Al-Li phase diagram. Lines: binodals (solid), metastable fcc-L₁₂ binodals (dashed).

for the IPB calculations we have kept the lattice parameter fixed at 0.4 nm and ignored positional deviations from fcc lattice positions. This is valid because in Al-rich alloys, Al and Li have the same partial molar volumes which indicates that the relaxations are very small. For example, when the *c/a* ratio of the tetragonal Al₃Li DO₂₂ phase is computed, a value of 1.974 is found which differs insignificantly from the ideal ratio of 2. The *c/a* relaxation in this phase decreases the total energy by a paltry 0.0125 mRyd/atom. Hence, the approximation of ignoring deviations from the exact fcc lattice positions is well-justified in Al-rich alloys.

The phase equilibria at non-zero temperature were determined with the Helmholtz free energy

$$F^\alpha = E^\alpha - TS^\alpha \quad (5)$$

where *T* and *S* are the temperature and entropy, respectively. The tetrahedron approximation of the CVM was found to be insufficient to accurately represent the states of order and the associated energies of formation. Instead, the tetrahedron-octahedron maximal clusters [15] were used. The CVM equations were solved with the Newton-Raphson technique as described previously [9].

3. Results

The solid state part of the Al-Li phase diagram (see figure 2) has been computed from 1st principles with ECI which were obtained with eq. 2. Details concerning this CVM calculation will be published elsewhere [16] and an explanation of the various phases can be found in Ref. [17]. Considering that no adjustable, or fitted, parameters entered in this computation, the agreement with the assessed fcc - δ' (L₁₂) phase equilibrium [18] is remarkable (see dashed lines in figures 2 and 3). Moreover, in a recent study of the pressure dependence of this phase equilibrium [16] very good agreement with experimental results [19] was found too.

Based on the small error of the predicted formation energy, and the accurate representation of the fcc - δ'

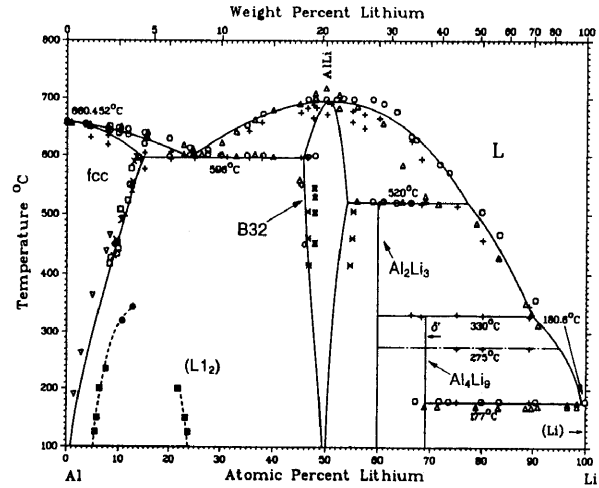


Figure 3: The assessed Al-Li phase diagram (from Ref. [18]). Lines: binodals (solid), metastable fcc-L₁₂ binodals (dashed).

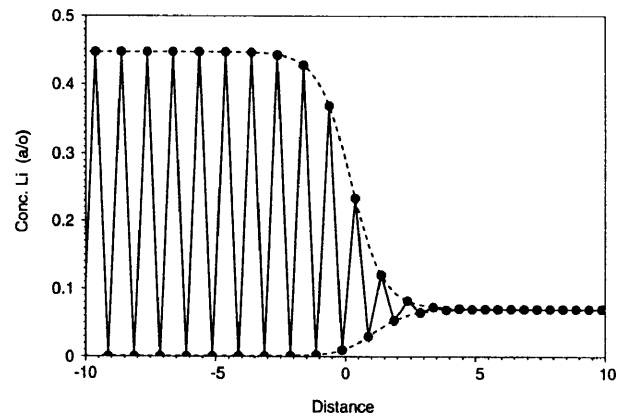


Figure 4: Li concentration averaged over (100) planes parallel to the IPB as a function of distance (in units of the lattice parameter) at 400 K as computed with the CVM. The solid line is drawn as a guide for the eye only.

(L₁₂) phase equilibrium, it is reasonable that the IPB between the Al fcc matrix and the δ' precipitate phase can be modeled accurately.

Figure 4 displays the computed composition profile across a (100) IPB at a temperature of 400 K. On the left the alternating occupancy of the (100) planes of the ordered δ' phase stands out and on the right the disordered solid solution in which all (100) planes have the same composition can be recognized easily. The transition region extends over about 12 consecutive (100) planes, or about 2.4 nm. When the calculation is repeated for various Li-concentrations in the supercell, the composition profile can be obtained as a continuous curve (dashed lines in figure 4). Within the context of a continuum theory, Cahn and Hilliard have shown that such a composition profile for a phase separating system has a sigmoid shape corresponding to an arctanh positional dependence [2]. We confirm that result, even though the discreteness of the lattice is taken into

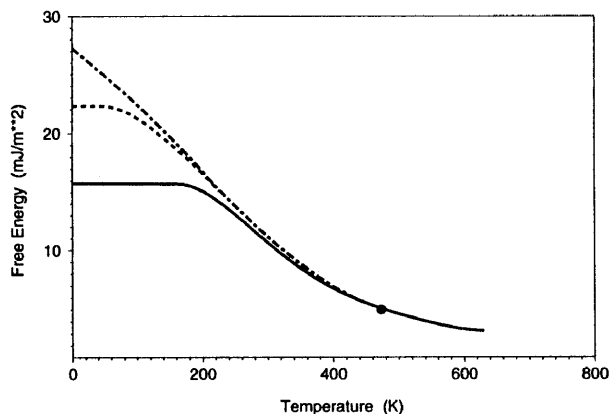


Figure 5: Interphase free energy as a function of temperature. Solid, dashed, and chain-dashed lines designate (100), (110), and (111) orientations as computed with the CVM, respectively, and the circle indicates a recent assessment [20] of experimental data for arbitrary orientations.

account. In contrast to the phase separation case, the width [2] of the IPB is a linear function of temperature and it does not diverge at the transition temperature. The origin of the finite width at the transition temperature is the fact that the fcc and $L1_2$ (δ') phases are related by a first- rather than second order phase transformation at the transition temperature [4].

In the absence of elastic energy terms, the orientational dependence of the IPB free energy determines the shape of precipitates. Such is the case in Al-Li alloys where coherence strains surrounding δ' precipitates are negligible.

Figure 5 shows the IPB free energy for three low index orientations as a function of temperature. Clearly, at temperatures where diffusion allows the formation of precipitates (roughly 300 K and above) the IPB free energy is virtually perfectly isotropic, which confirms a continuum result [2]. Hence, these first-principles calculations indicate that δ' precipitates are perfectly spherical, as is observed in actual alloys. Furthermore, our calculations show that in contrast to the dense packed (111) IPB, the (100) and (110) IPBs do not contribute any configurational excess entropy until some finite temperature is reached. This indicates that the (100) and (110) IPBs maintain zero-temperature type sharp composition profiles, whereas the (111) orientation has a disordered interface region even at very low temperature. At the order-disorder temperature the IPB free energy remains finite, which is due to the first order transformation between the fcc and $L1_2$ phases [4]. The numerical values of the ab-initio IPB free energy at a temperature of 473 K agree very well with a recent assessment of experimental results [20].

The excess configurational entropy associated with a (100) IPB is shown in figure 6. Clearly, this entropy cannot be assumed to be simply constant or linear with temperature. At very low temperature the (100) IPB

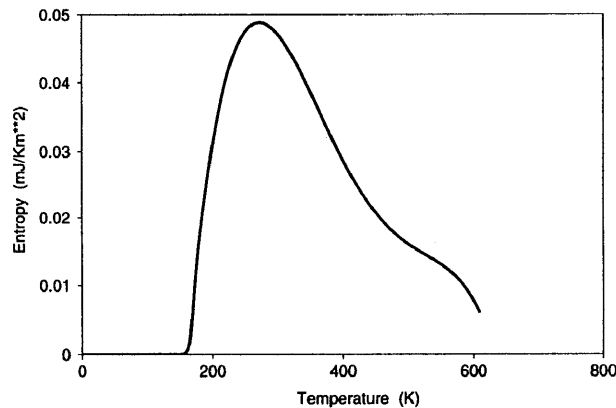


Figure 6: Interphase entropy of the (100) IPB as a function of temperature as computed with the CVM.

has zero width, and no extra compositional disorder is introduced. At very high temperature the fcc solid solution and the ordered phase have rather large configurational entropies themselves and the finite width IPB contributes little to the entropy. Only at the intermediate temperatures, where the solid solution still has low Li solubility, and where the ordered phase is still nearly perfectly ordered, does the disordered transition region in the IPB contribute significant excess entropy.

4. Summary

Summarizing: it has been shown that the thermodynamic properties of IPBs can be computed ab initio and the results agree well with the recently assessed experimental value. This means that now a link has been established between ab initio electronic total energy formalism and the theory of nucleation and growth.

Acknowledgements

The authors thank Dr M. van Schilfgaarde for providing an LMTO-ASA computer code and the Computer Center of IMR-Tohoku University for making a Hitachi S-3800 supercomputer available. Work at Sandia supported by the U.S. Department of Energy, Office of Basic Energy Sciences, Materials Science Division.

- 1) J.D. Van Der Waals, *Verhandel. Koninkl. Akad. Wetenschap. Amsterdam, Afdeel. Natuurk. Sect. I*, (1893); English translation in *J. Stat. Phys.* **20**, 197-244 (1979).
- 2) J.W. Cahn and J.E. Hilliard, *J. Chem. Phys.* **28**, 258-267 (1958).
- 3) R. Kikuchi and J.W. Cahn, *Acta Metall.* **27**, 1137-1353 (1979); and references cited therein.
- 4) A. Finel, in *Statics and Dynamics of Alloy Phase Transformations*, ed. by P.E.A. Turchi and A. Gonis, NATO ASI Series B: Physics Vol. **319**,

- Plenum, New York, 1993), pp. 495-540; and references cited therein.
- 5) A. Finel, V. Mazauric, and F. Ducastelle, *Phys. Rev. Lett.* **65**, 1016-1019 (1990).
 - 6) M. Sluiter, K. Esfarjani, and Y. Kawazoe, *Phys. Rev. Lett.* **75**, 3142-3145 (1995).
 - 7) H.L. Skriver, *The LMTO method*, Springer series in Solid State Science, Vol. **41**, (Springer, Heidelberg, 1983).
 - 8) J.W. Connolly and A.R. Williams, *Phys. Rev. B* **27**, 5169 (1983).
 - 9) M. Sluiter, D. de Fontaine, X.Q. Guo, R. Podloucky, and A.J. Freeman, *Phys. Rev. B* **42**, 10460 (1990).
 - 10) G.D. Garbulski and G. Ceder, *Phys. Rev. B* **51**, 67 (1995).
 - 11) G. Ceder, G.D. Garbulski and P.D. Tepesch, *Phys. Rev. B* **51**, 11257 (1995).
 - 12) M.J. Richards and J.W. Cahn, *Acta Metall.* **19**, 1263 (1971).
 - 13) S.M. Allen and J.W. Cahn, *Scripta Metall.* **7**, 1261 (1973).
 - 14) J. Kanamori and Y. Kakehashi, *J. Phys. (Paris), Colloq.* **38**, C-7-274 (1977).
 - 15) T. Mohri, J.M. Sanchez, and D. de Fontaine, *Acta Metall.* **33**, 1171 (1985).
 - 16) M. Sluiter, Y. Watanabe, D. de Fontaine, and Y. Kawazoe, submitted to *Phys. Rev. B* (1995).
 - 17) J.L.C. Daams, P. Villars, and J.H.N. van Vucht, *Atlas of Crystal Structures for Intermetallic Phases*, (ASM International, Materials Park OH, 1991).
 - 18) A.J. McAlister, *Bull. Alloy Phase Diagrams* **3**, 177 (1982).
 - 19) A. Matsumuro, K. Sakai, M. Senoo, *J. Mater. Sci.* **28**, 6567 (1993).
 - 20) J.J. Hoyt and S. Spooner, *Acta Metall. Mater.* **39**, 689-693 (1991); and references cited therein.